BRIEF COMMUNICATIONS

The purpose of this Brief Communications section is to present important research results of more limited scope than regular articles appearing in Physics of Fluids. Submission of material of a peripheral or cursory nature is strongly discouraged. Brief Communications cannot exceed four printed pages in length, including space allowed for title, figures, tables, references, and an abstract limited to about 100 words.

Reduction of flow-induced forces on a circular cylinder using a detached splitter plate

Jong-Yeon Hwang, Kyung-Soo Yang,[a] and Seung-Han Sun
Department of Mechanical Engineering, Inha University, Incheon, 402-751, Korea

(Received 22 November 2002; accepted 25 April 2003; published 2 July 2003)

Control of flow-induced forces on a circular cylinder using a detached splitter plate is numerically studied for laminar flow. A splitter plate with the same length as the cylinder diameter is placed horizontally in the wake region. Suppressing the vortex shedding, the plate significantly reduces drag force and lift fluctuation; there exists an optimal location of the plate for maximum reduction. However, they sharply increase as the plate is placed further downstream of the optimal location. This trend is consistent with the experimental observation currently available in the case of turbulent wake. © *2003 American Institute of Physics.* [DOI: 10.1063/1.1583733]

A splitter plate has been widely used for passive control of vortex shedding past a circular cylinder, resulting in considerable drag reduction.[1–6] However, main emphasis in most of the research on this topic has been placed on the flow control using splitter plates attached to the rear base point of the cylinder. Recently, an experimental study[7] was carried out for turbulent-wake control past a circular cylinder by means of a splitter plate with the same length as the cylinder diameter (d) placed in the wake region downstream of the cylinder (hereafter called ''detached'' splitter plate). In the experiment, drag coefficient (C_D) of the cylinder, Strouhal number (St) of vortex shedding, and negative of base suction coefficient ($-C_{pb}$) all decrease as the distance (G) between the rear base point of the cylinder and the leading edge of the splitter plate increases. However, when the plate was placed near a downstream location of $G/d=2.3$, a sudden increase in those quantities was noticed.[7]

In this investigation, a parametric study using numerical simulation is employed for two-dimensional (2D) laminar flow in order to clarify the flow physics related to the gradual reduction of the flow-induced forces on a circular cylinder and the subsequent sudden increase over a critical G/d. The incompressible continuity and momentum equations were used as the governing equations,

$$\frac{\partial u_j}{\partial x_j}=0 \quad (j=1,2), \tag{1}$$

$$\frac{\partial u_i}{\partial t}+u_j\frac{\partial u_i}{\partial x_j}=-\frac{\partial p}{\partial x_i}+\frac{1}{\mathrm{Re}}\frac{\partial^2 u_i}{\partial x_j \partial x_j} \quad (i,j=1,2), \tag{2}$$

where u_i is the velocity vector of which components are u and v in the x (streamwise) and y (normal) directions, respectively; p and Re denote pressure and Reynolds number based on the freestream velocity (U_∞) and d, respectively. The governing equations are discretized using a finite-volume method in a generalized coordinate system. Spatial discretization is second-order accurate. A hybrid scheme is used for time advancement; nonlinear terms and cross diffusion terms are explicitly advanced by a third-order Runge–Kutta scheme, and the other terms are implicitly advanced by the Crank–Nicolson method. A fractional step method[8] is employed to decouple the continuity and momentum equations. The Poisson equation resulted from the second stage of

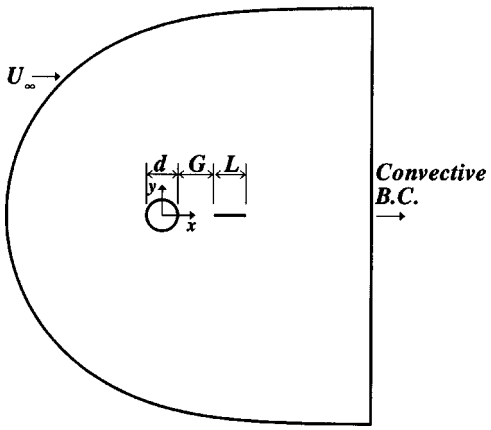

FIG. 1. Schematic diagram of the computational domain.

[a]Author to whom correspondence should be addressed. Electronic mail: ksyang@inha.ac.kr

TABLE I. Comparison with other authors' simulations at various Re; *a*, present study; *b*, Kwon and Choi (Ref. 5); and *c*, Park *et al.* (Ref. 10).

	With splitter ($G/d=0$) Re=100		Re=160		Without splitter Re=100	
	a	*b*	*a*	*b*	*a*	*c*
C_D	1.17	1.18	1.08	1.10	1.34	1.33
St	0.137	0.137	0.156	0.155	0.167	0.164
B_s	3.21	3.21	2.75	2.74	1.36	1.37

the fractional step method is solved by a multigrid method. The length of the splitter plate (L) is fixed as $L=d$, and three cases of Re are considered (Re=30,100,160).

Figure 1 shows the entire computational domain along with the coordinates. A C-type grid system was employed for resolving the wake region efficiently. The computational domain occupies $-50d \leqslant x \leqslant 60d$ and $-50d \leqslant y \leqslant 50d$. It turned out that this domain size is large enough to prevent the outer and exit boundaries from affecting important flow quantities such as C_D and St for the range of Re considered in this study. The numerical resolution was determined by a rigorous grid-refinement study; 609 computing cells were allocated along the branch-cut and the cylinder surface with 121 cells in the corresponding perpendicular direction. A Dirichlet boundary condition ($u=U_\infty, v=0$) is imposed at the outer boundary excluding the exit, while a convective boundary condition[9] is used at the exit. All solid surfaces are treated as no-slip. The code was verified by comparing the values of the key physical quantities with those of other authors;[5,10] they are summarized in Table I where $C_D = D/(\frac{1}{2}\rho U_\infty^2 d)$, $\mathrm{St}=fd/U_\infty$, and B_s is the time-averaged length of the bubble behind the cylinder. Here, D, f and ρ represent time-averaged drag on the circular cylinder per unit depth, frequency of vortex shedding and fluid density, respectively.

Variation of C_D with G/d is presented in Fig. 2. In the case of steady flow (Re=30), the drag monotonically decreases as G/d increases; the amount of reduction in C_D is minimal. In the case of unsteady flow (Re=100,160), however, the drag slightly increases for $0 \leqslant G/d \leqslant 0.25$, and then monotonically decreases up to $G/d=2.6$. The higher Re is, the bigger the drag reduction is; one can get 3.0% drag reduction for Re=100, and 6.4% for Re=160 at the optimal location of the plate ($G/d=2.6$) compared with the case of an ''attached'' splitter plate ($G/d=0$). Compared with the case of no splitter plate, the corresponding drag reductions

FIG. 2. Variation of drag coefficient (C_D) with G/d; Re=30 (◇), Re=100 (□), Re=160 (▽).

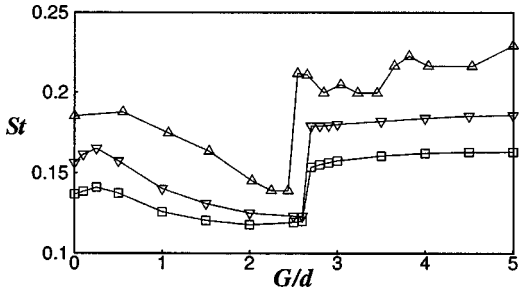

FIG. 3. Variation of Strouhal number (St) with G/d; Re=100 (□), Re=160 (▽). Experimental data of Ozono (Ref. 7) at Re=6.7×10^3 (△). The length of the splitter plate is the same as the diameter of the cylinder.

are 14.7% and 23.1% for Re=100 and Re=160, respectively. The increase of C_D for small G/d is due to the fact that the pressure near the rear base point of the cylinder rather drops when the gap is small. One can also notice a sudden increase of C_D between $G/d=2.6$ and $G/d=2.7$. After that, the effect of the splitter plate drastically diminishes; C_D asymptotically approaches the value without the splitter plate. It can be speculated that these phenomena in unsteady flow must be related to vortex shedding that steady flow does not have. In fact, it turned out that is the case as explained later. A similar trend is also found in St as Fig. 3 indicates. The gradual decrease of St for $0.25 < G/d < 2.6$ implies suppression of vortex shedding by the splitter plate. It is interesting to note that turbulent wake exhibits a similar behavior. The sudden increase of St near $G/d=2.6$ also implies a significant change in the pattern of vortex shedding beyond that location of the splitter plate.

Figure 4 presents variation of the base suction coefficient with G/d; its negative values are plotted for convenience sake. The base suction coefficient is defined as

$$C_{pb}=(P_b-P_o+\tfrac{1}{2}\rho U_\infty^2)/\tfrac{1}{2}\rho U_\infty^2, \tag{3}$$

where P_o and P_b represent time-averaged pressures at the front stagnation point and at the base point of the cylinder, respectively. The trend of $-C_{pb}$ is similar to that of C_D or St; the numerical data are consistent with Ozono's experiment[7] for turbulent wake of the same flow configuration. Since the form drag is dominant over the viscous drag, the strong correlation between $-C_{pb}$ and C_D implies that the

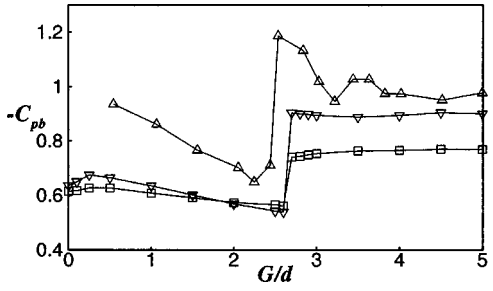

FIG. 4. Variation of the base suction coefficient (C_{pb}) with G/d; its negative values are plotted for convenience sake. Re=100 (□), Re=160 (▽). Experimental data of Ozono (Ref. 7) at Re=6.7×10^3 (△). The length of the splitter plate is the same as the diameter of the cylinder.

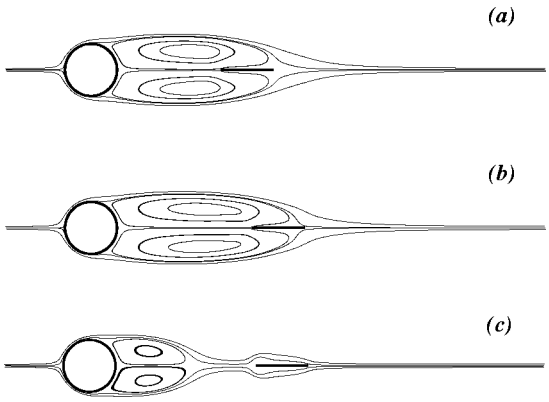

FIG. 5. Time-averaged streamlines for the unsteady flow at Re=100; (a) $G/d=2.0$, (b) $G/d=2.6$, and (c) $G/d=2.7$.

drag reduction for $0.25<G/d<2.6$ is achieved by the pressure increase on the rear surface of the cyliner including the base point. Similarly, the slight increase of drag for $0 \leqslant G/d \leqslant 0.25$ can be explained by that of $-C_{pb}$ for the same range of G/d. It should be also noted that in Fig. 4 the reduction of $-C_{pb}$ (consequently C_D) in turbulent wake before its sudden increase is much larger than the laminar counterparts. This is also consistent with the fact that the reduction at higher Re is larger than that of low-Re case in laminar flow. Compare the two Re cases in Fig. 4.

The instantaneous lift force is also significantly affected by the splitter plate. The fluctuation of lift force is considerably reduced by the splitter plate; the maximum reduction of lift fluctuation also occurs at $G/d=2.6$ with reduction rates

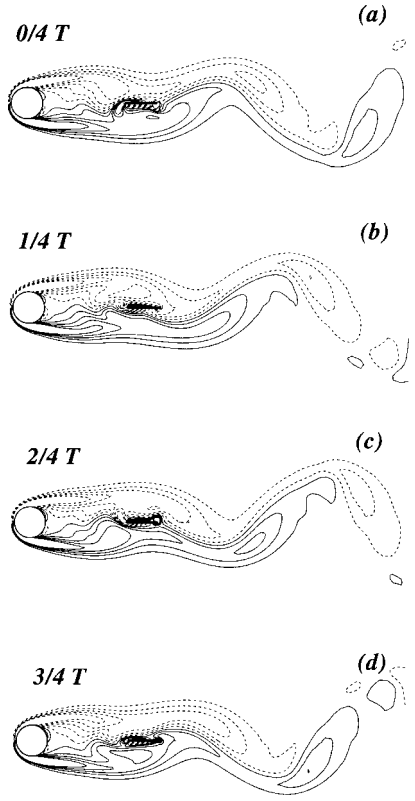

FIG. 6. Instantaneous spanwise vorticity (ω) contours at equal intervals during one period of vortex shedding, Re=160, $G/d=2.6$. Here, T is the period of vortex shedding, and $\Delta\omega d/U_\infty=0.56$.

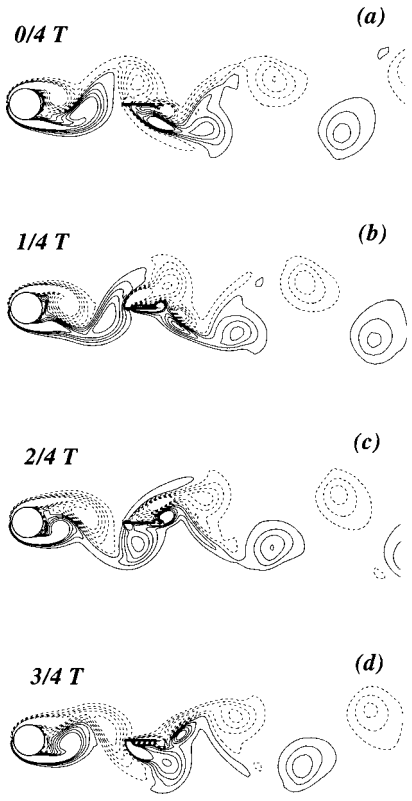

FIG. 7. Instantaneous spanwise vorticity (ω) contours at equal intervals during one period of vortex shedding, Re=160, $G/d=2.7$. Here, T is the period of vortex shedding, and $\Delta\omega d/U_\infty=0.56$.

of 43.0% compared with that of $G/d=0$, and 86.8% compared with the case without a splitter plate.[10]

Figure 5 presents time-averaged streamlines for the unsteady flow at Re=100 for various cases of G/d. In the case of the steady flow, the size of the rear bubble does not significantly depend upon the location of the splitter plate. That is not the case for unsteady flow; the rear bubble gets bigger as the splitter plate is placed further downstream [Figs. 5(a) and 5(b)] until $G/d=2.6$ at which the drag and lift fluctuation are minimal. The bubble suddenly shrinks between $G/d=2.6$ and $G/d=2.7$, and remains little changed for further downstream locations of the splitter plate. From these observations, one can conjecture that the significant reductions of drag and lift fluctuation achieved in unsteady flows using a ''detached'' splitter plate are strongly related to suppression of the vortex shedding near the circular cylinder.

Instantaneous spanwise vorticity (ω) contours for Re =160 at equal intervals during one period of vortex shedding are presented in Figs. 6 and 7 at $G/d=2.6$ and $G/d=2.7$, respectively. The solid and dashed lines represent positive and negative values, respectively. In Fig. 6 where the splitter plate is placed at the critical distance ($G/d=2.6$), the splitter plate effectively suppresses vortex shedding near the circular cylinder; the separated free-shear layers do not interact with each other. Consequently, the pressure on the rear surface of the cylinder rises, resulting in significant reduction of drag force. Furthermore, the vorticity field between the cylinder and the splitter plate remains quasi-symmetric with respect to the x axis in time. This implies quasi-symmetry of the pressure distribution in the normal direction on the cylinder

surface, resulting in significant reduction of lift fluctuation. Vortex shedding occurs past the splitter plate.

When the splitter plate is located just beyond the critical distance, a drastic change in the flow field is noticed (Fig. 7). The separated free-shear layers downstream of the cylinder become unstable, resulting in the alternating and periodic vortex shedding. Thus the ''favorable'' instantaneous pressure distribution described above no longer holds, and the pressure field in the vicinity of the cylinder suddenly changes closely to that of the case without the splitter plate, resulting in large drag force and lift fluctuation. One can also notice that the two vortex sheddings past the cylinder and past the splitter plate are completely synchronized with $\mathrm{St}=0.179$. Compare Fig. 7(a) with Fig. 7(c). The splitter plate, however, still interferes with the vortex shedding past the cylinder; see Fig. 7(b) or 7(d). As a result, the value of Strouhal number without the splitter plate at $\mathrm{Re}=160$ ($\mathrm{St}=1.88$) is slightly larger than the synchronized value ($\mathrm{St}=0.179$) of $G/d=2.7$.

As indicated by the numerical results presented above, a ''detached'' splitter plate can play an important role in reducing flow-induced forces on a circular cylinder. Flow mechanisms responsible for the reductions of drag force and lift fluctuation have been identified for laminar flow. It remains to be further investigated how the ''detached'' splitter plate affects the flow-induced forces on a cylinder in the case of turbulent flow. Nevertheless, a ''detached'' splitter plate appears to be one of the effective ways in passive control of the flow-induced forces.

ACKNOWLEDGMENT

This work was supported by Inha University Research Grant No. INHA-22664.

[1] E. A. Anderson and A. A. Szewczyk, ''Effect of a splitter on the near wake of a circular cylinder in 2 and 3-dimensional flow configurations,'' Exp. Fluids **23**, 161 (1997).
[2] C. J. Apelt and G. S. West, ''The effect of wake splitter plates on bluff-body flow in the range $10^4<R<5\times10^4$: Part 2,'' J. Fluid Mech. **71**, 145 (1975).
[3] M. F. Unal and D. Rockwell, ''On vortex formation from a cylinder. Part 2. Control by splitter-plate interference,'' J. Fluid Mech. **190**, 513 (1987).
[4] C. J. Apelt, G. S. West, and A. Szewczyk, ''The effect of wake splitter plates on the flow past a circular cylinder in the range $10^4<R<5\times10^4$,'' J. Fluid Mech. **61**, 187 (1973).
[5] K. Kwon and H. Choi, ''Control of laminar vortex shedding behind a circular cylinder using splitter plates,'' Phys. Fluids **8**, 479 (1996).
[6] E. Rathakrishnan, ''Effect of splitter plate on bluff body drag,'' AIAA J. **37**, 1125 (1999).
[7] S. Ozono, ''Flow control of vortex shedding by a short splitter plate asymmetrically arranged downstream of a cylinder,'' Phys. Fluids **11**, 2928 (1999).
[8] M. Rosenfeld, D. Kwak, and M. Vinokur, ''A fractional-step method for the unsteady incompressible Navier–Stokes equations in generalized coordinate systems,'' J. Comput. Phys. **94**, 102 (1994).
[9] L. L. Pauley, P. Moin, and W. C. Reynolds, ''A numerical study of unsteady laminar boundary layer separation,'' Report No. TF-34, Thermosciences Division, Department of Mechanical Engineering, Stanford University (1988).
[10] J. Park, K. Kwon, and H. Choi, ''Numerical solutions of flow past a circular cylinder at Reynolds numbers up to 160,'' KSME Int. J. **12**, 1200 (1998).